Structural evolution of Fe-Al multilayer thin films for different annealing temperatures

2001 J. Phys.: Condens. Matter 13 811

(http://iopscience.iop.org/0953-8984/13/5/303)

INSTITUTE OF PHYSICS PUBLISHING JOURNAL OF PHYSICS: CONDENSED MATTER

J. Phys.: Condens. Matter **13** (2001) 811–821 www.iop.org/Journals/cm PII: S0953-8984(01)18002-1

Structural evolution of Fe–Al multilayer thin films for different annealing temperatures

R Checchetto[1,3], C Tosello[1], A Miotello[1] and G Principi[2]

[1] Istituto Nazionale per la Fisica della Materia (INFM) and Dipartimento di Fisica dell'Università di Trento, I-38050 Povo (TN), Italy
[2] Istituto Nazionale per la Fisica della Materia (INFM) and Dipartimento di Ingegneria Meccanica dell' Università di Padova, I-35131 Padova, Italy

E-mail: checchet@science.unitn.it

Received 13 October 2000, in final form 21 December 2000

Abstract

The phase formation during thermal annealing of Fe/Al multilayer thin films prepared by electron-beam evaporation, with an overall atomic concentration ratio of Fe:Al = 1:1, has been studied by Rutherford backscattering spectrometry (RBS), x-ray diffraction spectroscopy (XRD), and conversion-electron Mössbauer spectroscopy (CEMS). At the annealing temperature of 473 K some degree of atomic mixing between Fe and Al layers is revealed only by CEMS. At 573 K a large degree of atomic mixing is indicated also by RBS, leading to the nucleation and growth of the B2 FeAl intermetallic phase, as detected by means of XRD and CEMS. At 673 K all Fe atoms have reacted and the multilayer film is transformed into a defective B2 phase. Annealing at higher temperature increases the structural order of the B2 phase. We suggest that the observed phase formation occurs in three stages: (1) formation of a thin intermixed layer between Fe and Al in the as-deposited sample; (2) Al migration into the initial intermixed layer; (3) B2 phase growth at the interface between the intermixed layer and the Fe layer.

1. Introduction

Among the systems forming intermetallic compounds, Fe–Al has been particularly intensively studied. Detailed reviews of the available experimental data and thermodynamic properties, overviews on properties and applications, and conference proceedings are available in the literature [1–5]. In the iron-rich side of the Fe–Al phase diagram, which is of technological interest, four different single-phase areas can be distinguished:

(1) the α-Fe phase (A2), a disordered solid solution based on bcc Fe where Al can be dissolved up to a concentration of 20 at.% at room temperature;

[3] Author to whom any correspondence should be addressed.

0953-8984/01/050811+11$30.00

(2) the γ-Fe phase, a disordered solid solution based on fcc Fe with Al dissolved at a concentration <1.3 at.%;
(3) the ordered FeAl phase with the CsCl cubic structure (B2) forming through ordering of α-Fe; and
(4) the ordered Fe_3Al phase with the BiF_3 structure (DO_3) forming through a second-order phase transformation from FeAl [1].

Iron aluminides based on the Fe_3Al and the FeAl structures are particularly interesting, being candidate high-temperature structural materials. These materials have, in fact, low cost and good wear resistance, density lower than that of the commercial high-temperature structural materials, and excellent resistance to oxidation, sulphidation, and corrosion [3, 4].

Intermetallic phases formed by solid-state reactions in thin-film structures play an important role from a technological point of view because of their applications, ranging from use as heat- and corrosion-resistant coatings for bulk materials [6, 7] to use as metallization layers in microelectronic devices [8, 9]. In particular, Fe–Al-based alloy films, such as Fe–Al–Si (Sendust alloy) and Fe–Al–Si–Ni (Supersendust alloy), have been widely used as magnetic recording head materials because of their soft magnetic and good mechanical properties [10–12].

Recently, many interesting papers have been published dealing with the structural characterization of the intermixing between Fe and Al layers in Fe/Al multilayers. Noetzel *et al* [13], analysing by means of conversion-electron Mössbauer spectroscopy (CEMS) and Rutherford backscattering spectrometry (RBS) Fe/Al multilayers deposited by pulsed laser deposition (PLD), observed that the intermixing of adjacent Fe and Al layers must be described in terms of ballistic effects, related to the high kinetic energy of Fe and Al particles, followed by chemical mixing. The authors obtained the interesting result that, depending on whether Fe is deposited on Al or Al on Fe, the formation of different phases occurs: in Fe-rich areas the formation of a bcc solid solution occurs, while in the Al-rich environment an amorphous phase is observed. Meyer *et al* [14] observed, in an x-ray absorption fine-structure (XAFS) examination of PLD multilayers, the presence of extended interface regions characterized by intermixing significantly larger for the deposition of Fe on Al than for the deposition of Al on Fe. Shao and Tsakiropoulos [15] deposited by means of an electron beam alternating layers of Fe and Al on a substrate at 640 K. The authors observed by transmission electron microscopy (TEM) and energy-dispersive x-ray (EDX) analysis that the formation of Fe–Al B2 phase occurred for large Fe-to-Al nominal thickness ratios, while the formation of Al-rich phases occurred for comparable thickness ratios of the deposited Al and Fe films.

In this paper we present an experimental study on the structural evolution of and phase formation induced by UHV thermal annealing in Fe/Al multilayer thin films having an average atomic composition of 1:1. Our purpose is to identify the compounds formed in the low-temperature ($T < 773$ K) solid-state reaction among those indicated in the Fe–Al phase diagram, and to clarify the role played by the chemical driving forces and kinetic processes in the interaction of the multilayer system. Starting from the as-deposited multilayer system, the formation of the B2 FeAl phase is followed in detail. Then, its thermal stability and defect evolution is studied.

2. Experimental procedure

Fe–Al multilayers were deposited on (100)-oriented Si wafers by sequential evaporation of 15 couples of 10 nm Fe and 14 nm Al bilayers: in view of the fact that the Fe and Al atomic density are 0.85×10^{23} atoms cm^{-3} and 0.6×10^{23} atoms cm^{-3}, respectively, the thickness of

each metallic layer was chosen to ensure an average 1:1 atomic composition of the deposited multilayer sample. The deposition process started with the Fe layer and ended with the Al layer, in order to increase the multilayer adhesion to the silicon substrate and to limit the surface oxidation. The layers were deposited by means of an electron beam from two different crucibles containing high-purity materials at a growth rate of approximately 0.1 nm s^{-1}, and the deposited thickness was monitored by oscillating quartz. During the deposition process the substrate temperature never exceeded 310 K. The background pressure remained in the low 10^{-6} Pa range.

In order to enhance the atomic mixing and to promote the formation of intermetallic Fe–Al phases, the deposited samples were transferred to an UHV heating chamber and subjected to annealing at temperatures ranging from 273 to 773 K.

RBS analysis was performed with the HVEC AN2000 Van de Graaf accelerator at Laboratori Nazionali di Legnaro by using a 2.0 MeV $^4He^+$ beam. In order to check the average atomic composition and the layered structure of the Fe–Al system, the RBS measurements were performed with the beam impinging at 0° and 60° angles, respectively, with respect to the normal to the surface of the sample analysed. The detector was placed at a 100° scattering angle.

XRD was used for the investigation of the structural evolution of the multilayer samples before and after the heat treatment. The measurement was carried out by a Philips PW 1771/00 diffractometer (tube voltage 40 kV; tube current 35 mA) by means of a θ–2θ scan between 20° and 140° with a $\Delta\theta = 0.05^\circ$ step using Cu Kα radiation ($\lambda = 1.540\,54$ Å).

The local environment of the Fe atoms in the as-deposited sample and after the heat treatments was studied by CEMS. The spectra were recorded at room temperature by using a conventional spectrometer with a flowing-gas proportional counter and a source of ^{57}Co of about 10 mCi in a Rh matrix. A standard least-squares-minimization routine was used to fit the spectra profiles as a superposition of Lorentzian lines.

3. Results

3.1. As-deposited sample

The XRD pattern in figure 1(a) of the as-deposited Fe–Al multilayer displays, besides the intense contribution of the Si substrate at $\sim 70^\circ$, only the Al (111) and α-Fe(110) peaks [16, 17] with a negligible contribution of the Al(200) peak. The Al and Fe grain sizes of 14 and 6 nm, respectively, estimated by Debye–Scherrer analysis, are typical of metallic thin films deposited at room temperature by an electron beam. Correspondingly, the CEM spectrum in figure 2 shows essentially a typical α-Fe sextet, rather broad (with a linewidth of about 0.35 mm s^{-1} compared to about 0.28 mm s^{-1} for bulk iron) and with an unresolved very weak central contribution, indicating a certain degree of interatomic mixing at the interfaces between Fe and Al layers. The RBS profile in figure 3(a), obtained with the He^+ beam impinging at a 60° angle, can resolve only the first three layers of Fe and the first two layers of Al. Simulation of the RBS spectrum taken with a 0° impinging angle, using the RUMP code [18], has confirmed the atomic average compositional ratio to be 1:1.

3.2. 473 K UHV annealing

The CEM spectrum in figure 2 of the sample annealed at 473 K for 240 min, if compared to that of the as-deposited sample, displays some differences: a broadening of the sextet, with the outer linewidths reaching about 0.50 mm s^{-1}, and the presence of a central doublet.

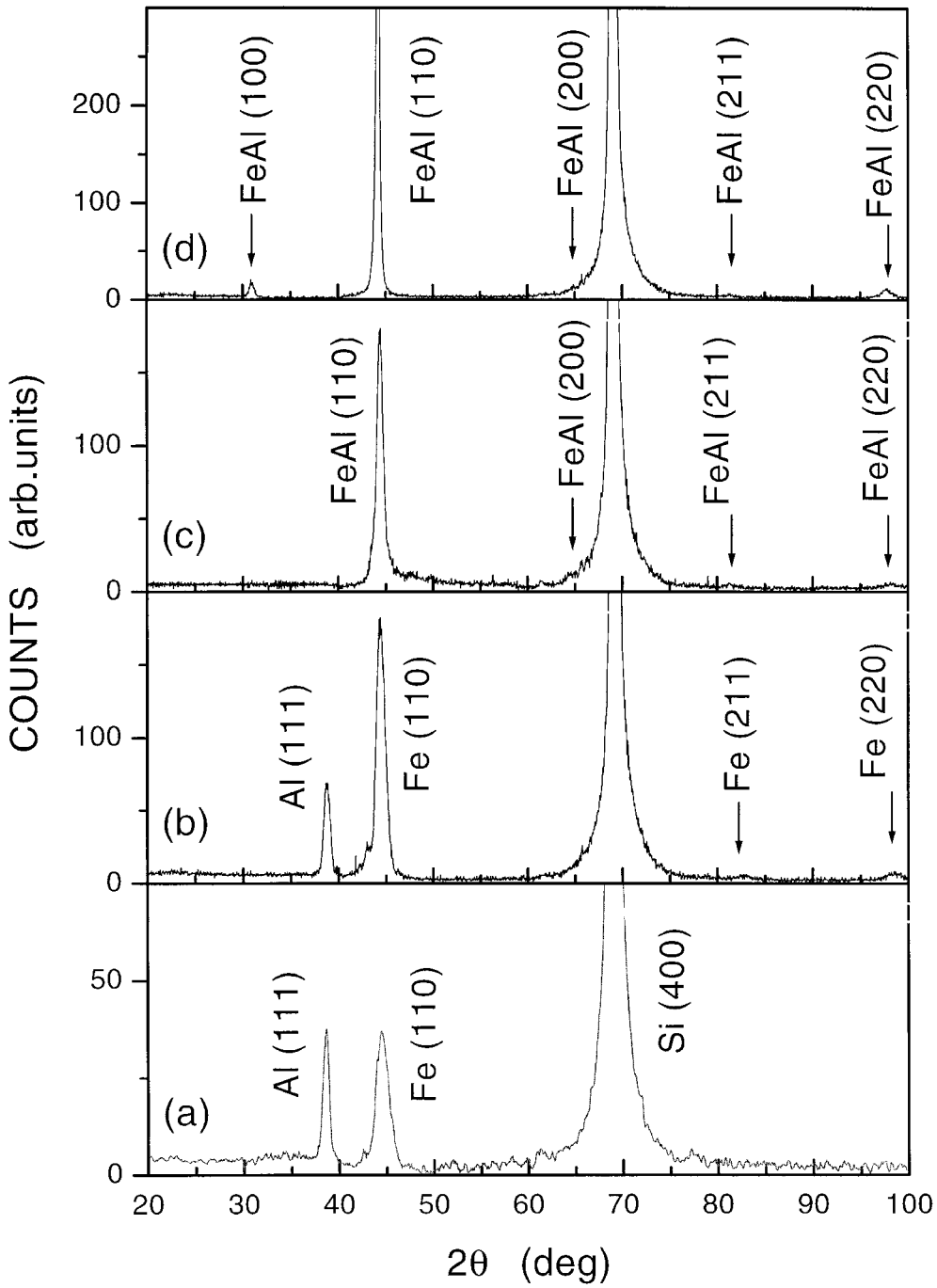

Figure 1. X-ray diffraction patterns of the Fe–Al multilayer as deposited and annealed at different temperatures.

These changes are due to partial atomic mixing at the interfaces between Fe and Al layers: the broadening of the sextet indicates diffusion of Al into the Fe bcc lattice, while the doublet

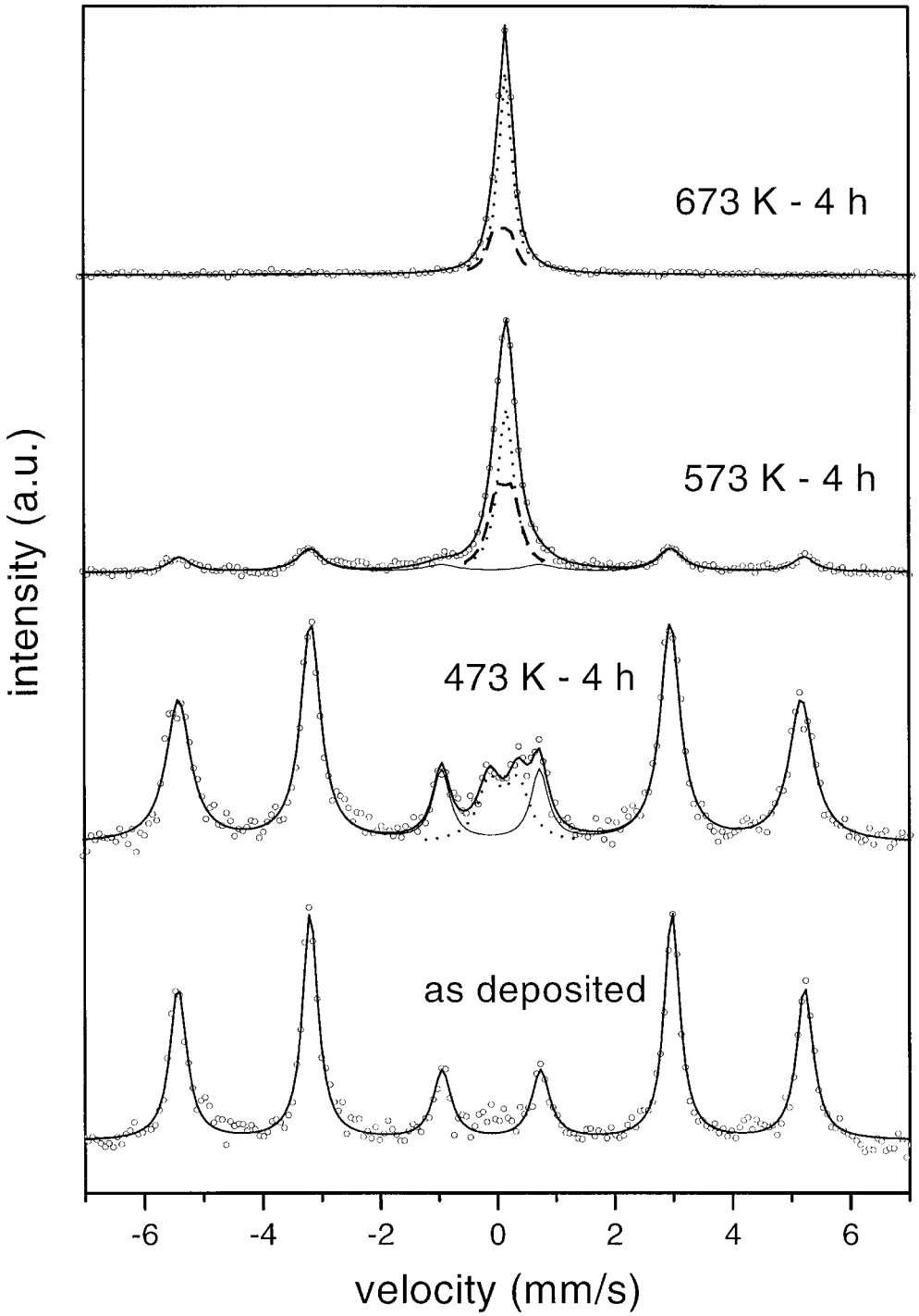

Figure 2. Mössbauer spectra of the Fe–Al multilayer as deposited and annealed at different temperatures. Key to symbols: open circles: data points; continuous thick line: best fit; continuous thin line: Fe atoms in Fe(Al) solid solution; dots: Fe atoms in Al-rich environment; short-dashed line: Fe atoms in ordered B2 FeAl; dashed line: Fe atoms in disordered B2 FeAl.

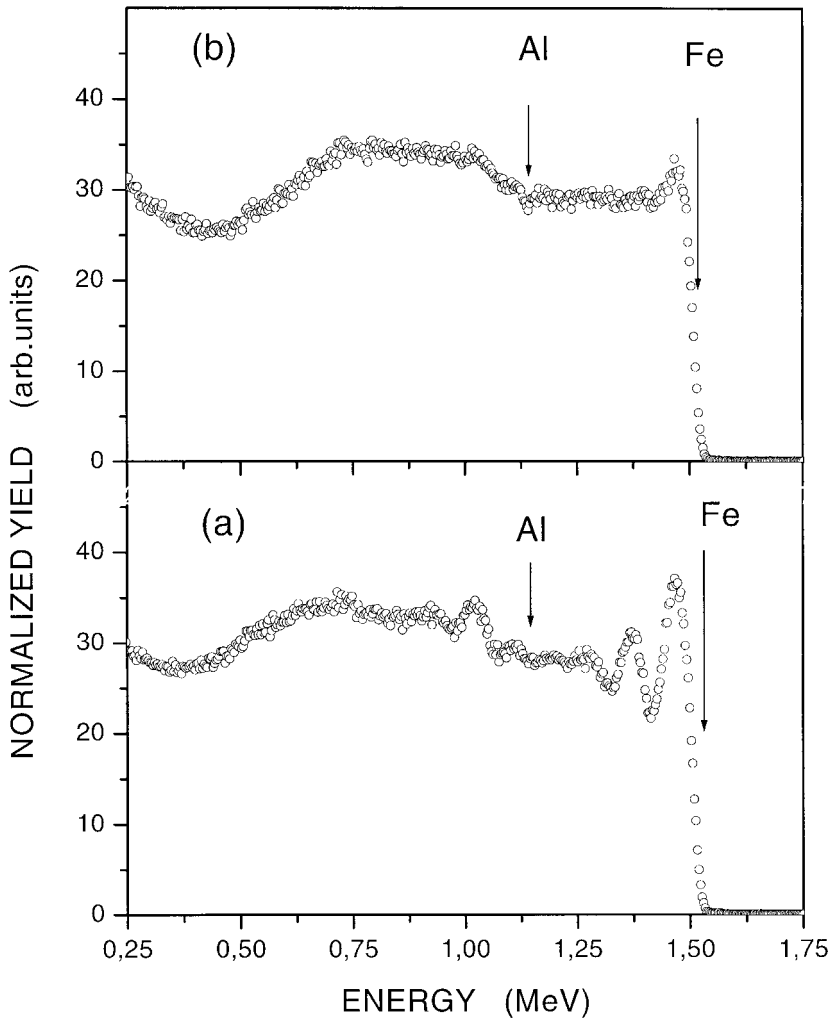

Figure 3. RBS spectra in tilted geometry of: (a) an as-deposited sample; (b) a sample annealed at 573 K.

having parameters (isomer shift of 0.23 mm s^{-1}, and quadrupole splitting of 0.48 mm s^{-1}) close to the ones characteristic of an Al-rich Fe–Al alloy [19] indicates that a proportion of the Fe atoms (at the interfaces with the Al layers) sit in an environment rich in Al atoms. This partial atomic mixing does not produce any characteristic Fe–Al peak in the XRD pattern of figure 1(b): we only notice the presence of the α-Fe(211) and α-Fe(220) reflections, indicating a better crystallization of the unmixed Fe atoms [16, 17].

3.3. 573 K UHV annealing

In the RBS spectrum of the sample annealed at 573 K for 240 min, figure 3(b), we notice a significant degree of atomic mixing between Fe and Al layers, even if pure Fe is still present, because we do not see any change in the edge of the Fe signal, which also maintains a peaked structure. The formation of a new crystalline phase, of the B2 FeAl type, is well evidenced by

the XRD pattern in figure 1(c), where all the peaks of Al disappear and those of Fe are slightly shifted, indicating alloying with Al [20]. Al_3Fe phase formation can be excluded because, even if the (004) Al_3Fe peak at $2\theta = 44.81^\circ$ could be confused with the (110) FeAl B2 one at $2\theta = 44.35^\circ$, the (222) and (440) reflections at $2\theta = 25.12^\circ$ and $2\theta = 24.16^\circ$, respectively, are not present. This evolution is also confirmed by the corresponding Mössbauer spectrum in figure 2, where the sextet of metallic iron is strongly reduced at the expense of a strong central peak. This peak can be deconvoluted into a singlet with an isomer shift of about 0.28 mm s^{-1} and an unresolved doublet with an isomer shift δ of about 0.20 mm s^{-1} and a quadrupole splitting of about 0.23 mm s^{-1}, corresponding to iron atoms in the B2 FeAl ordered phase and in defected positions, respectively.

3.4. 673 K UHV annealing

673 K UHV annealing for times ranging from 15 to 240 minutes has been performed in order to follow the phase formation kinetics. CEMS analysis has detected mixing also for short times. After a 240-minute treatment, all Fe atoms have reacted, as indicated by the vanishing of the sextet in the spectrum profile of figure 2. The complete disappearance of pure α-Fe is also confirmed by the RBS analysis which indicates a complete and homogeneous mixing of the atomic species.

The XRD pattern of figure 1(d) displays the peaks characteristic of the B2 FeAl crystalline structure, with relative intensities indicating a strong preferred orientation in the growth of the B2 phase [20]. The estimated grain size is of the order of 50 nm. The central peak in the CEM spectrum is deconvoluted, as in the previous spectrum, into a singlet with an isomer shift of 0.27 mm s^{-1} and a doublet with an isomer shift of 0.21 mm s^{-1} and a quadrupole splitting of 0.22 mm s^{-1}. The spectrum of the same sample, measured over a reduced velocity range, figure 4, allows a more detailed fitting. If we associate the doublet with iron atoms in the corners of Fe atoms in antisite positions, with 1:8 being the ratio between iron atoms in antisite positions (substituting for Al atoms) and iron atoms in corner antisite positions, we are justified in adding another singlet constrained to have the same isomer shift and linewidth of the doublet, but with a relative area in a ratio 1:8 to that of the doublet. This model describes very satisfactorily the spectral profile.

4. Discussion

4.1. Nucleation of the B2 phase

Solid-state reactions induced by thermal annealing in metal–metal thin-film systems produce phases which are driven by the chemical potential and the final compounds are those predicted by the phase diagram. However, the first step of the reaction seems to have no correlation with the thermodynamic properties of the system. Rothhaar *et al* [21], for example, deposited Al–Ni multilayer films with an average 1:1 atomic composition and observed that at 433 K the first nucleating phase was Al_3Ni. The thermodynamics, in contrast, indicates AlNi as the preferred phase, having -58.7 kJ mol^{-1} as the heat of formation (ΔH), lower than the value for Al_3Ni, -37.6 kJ mol^{-1} [2]. Bené [22] proposed, as an empirical rule, that the first phase nucleated in a metal–metal thin-film reaction at low temperature is the one immediately adjacent to the low-temperature eutectic in the binary phase diagram. This rule is verified for many binary systems, but it is not of general application. Majni *et al* [23], in fact, by studying the Au–Al system, observed that the first phase formed was Au_5Al_2, while Bené's rule indicates Au_4Al. These discrepancies reflect the fact that the phase diagram describes an equilibrium

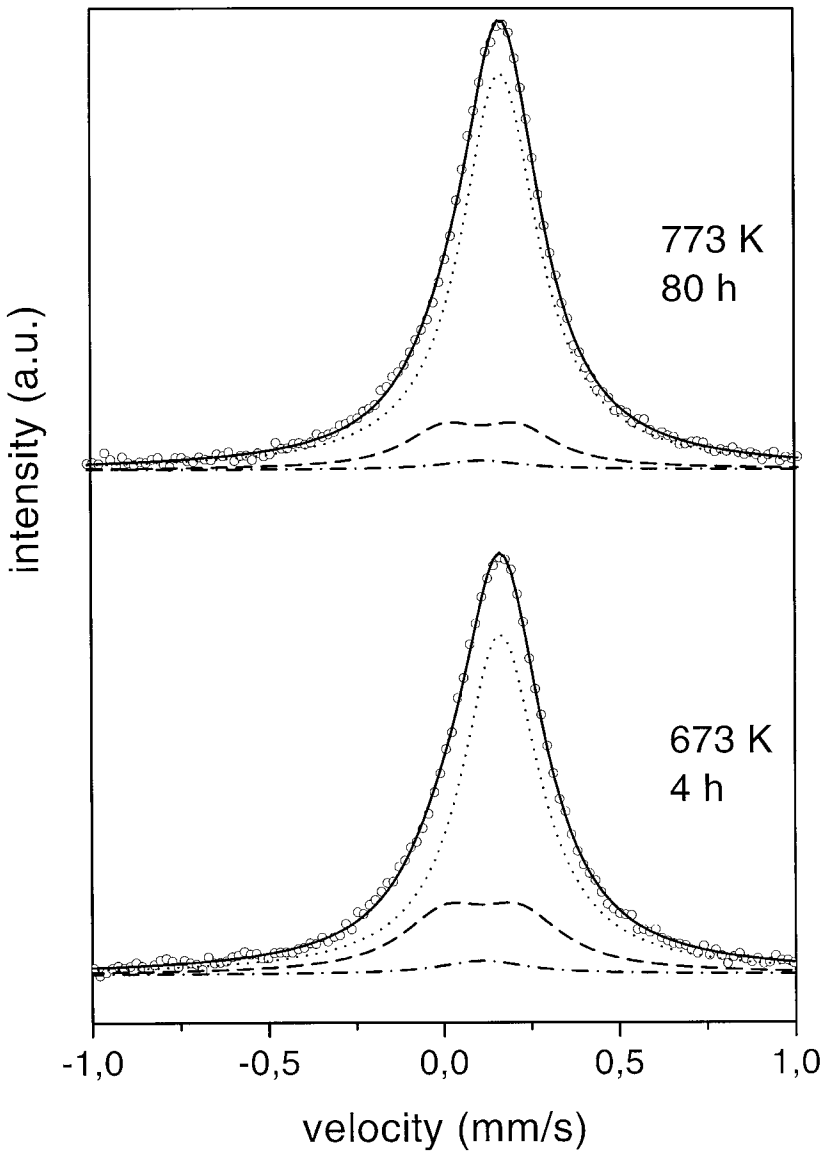

Figure 4. Mössbauer spectra of samples annealed as indicated: key to symbols: open circles: data points; continuous thick line: best fit; short-dashed line: Fe atoms in ordered B2 FeAl; dash–dotted line: Fe atoms in antisite positions; dashed line: Fe atoms in corner antisite positions.

condition, while for thin films a time dependence of the solid-state reaction is usually observed. Therefore, for the interpretation of the experimental data, it is necessary to consider the role of both the thermodynamic and kinetic processes involved on a nanometric scale.

The formation of the B2 FeAl phase in our multilayer system does not confirm Bené's rule, $FeAl_3$ being the phase near the low-temperature eutectic (925 K). From the thermodynamic point of view we cannot derive conclusions because the heat of formation of the Al-rich phases $FeAl_3$ ($\Delta H = -27.9$ kJ mol^{-1}), Fe_2Al_5 ($\Delta H = -27.0$ kJ mol^{-1}), and $FeAl_2$ ($\Delta H = -26.1$ kJ mol^{-1}) has quite similar values to that of the B2 phase, -25.1 kJ mol^{-1}

[2]. We suggest that the B2 FeAl phase formation and growth in the solid-state reaction can be explained by considering the composition of the mixed interface layer (MIL) during the deposition stage and the supply of the atomic elements to the MIL during the thermally enhanced solid-state reaction.

In the present as-prepared multilayer samples there is some degree of atomic mixing at the interfaces, as experimentally evidenced by the broad lines of the sextet and by the unresolved central component in the CEM spectrum in figure 2. This atomic mixing is favoured by chemical driving forces, the Fe–Al system having negative values of mixing enthalpy [1]. Moreover, from the phase diagram, we can find an indication of the composition of the mixed interlayer. It is known that the Al solubility in Fe is much higher than the Fe solubility in Al: at room temperature, Al can be dissolved up to 20 at.% in α-Fe, whereas the solubility of Fe in Al is lower than 0.04 at.% [1]. Geilman *et al* [24] in a CEMS analysis of Fe/Al multilayers deposited by thermal evaporation observed that the interface layer, a few nm thick, consisted of a structured region composed of a paramagnetic phase of approximately Fe:Al = 1:1 atomic composition and a solid solution of Al in Fe, presumably with a strong Al concentration gradient. By observing the increased intensity of the central component in the CEM spectrum of the sample annealed at 473 K, figure 2, we deduce that the atomic mixing is appreciable even for low-temperature treatment. The key point is to understand which is the role played by the mutual mobility of the atomic species supplied to the MIL, where the new phase nucleates.

An important indication can be obtained from the results of a CEMS study by Meyer *et al* [25] on the structural characterization of Fe–Al multilayers consisting of four ^{57}Fe (3.5 nm)/Al (22 nm) bilayers. As the sensitivity of the Mössbauer analysis of ^{57}Fe-enriched samples is very high, the authors pointed out that the MIL of the as-deposited sample consisted of a diluted solid solution of Al in Fe without the formation of any known Fe–Al compound and that in the first stage of atomic mixing the CEM spectrum indicated an increase of the Al concentration in this MIL diluted alloy region.

The nucleation of the B2 phase in our samples can be explained in terms of thermodynamic forces. In fact, the Al diffusion enriches the Fe bcc phase (A2) in Al in the MIL region and, beyond a certain Al concentration threshold, the nucleation of a new solid phase occurs. Among the B2 and DO_3 phases, indicated in the Fe-rich side of the Fe–Al phase diagram, the nucleation of the B2 phase is strongly favoured by thermodynamic forces. Their heats of formation are, in fact, -25.1 kJ mol^{-1} (B2) and -15.7 kJ mol^{-1} (DO_3), respectively [2].

Once the B2 phase is nucleated, its growth may be controlled by the diffusion of Fe atoms into the pure Al layer or Al atoms into the pure Fe layer through the intermetallic layers already formed. The growing phase acts thus as a diffusion barrier, which controls the supply of atomic elements to the intermetallic–metallic interface (B2/α-Fe and/or B2/Al) where the reaction occurs. This mechanism is rather common in thin-film reactions: in particular it was observed in the formation of silicides between Si and near-noble-metal films [26]. As an example, the growth of Ni_2Si is determined by the transport of mainly Ni through the silicide [27]. As suggested by a recent paper of Eggersmann and Mehrer [28] on the diffusion in the intermetallic phases of the Fe–Al system, the mobility of Al atoms both in A2 and in B2 Fe–Al phases is higher than the mobility of Fe atoms by at least a factor of 10 at 573 K. This result indicates that, after nucleation, the growth of the intermetallic B2 layers mainly occurs through solid-state reaction of Al atoms at the B2/α-Fe interface.

It is important to point out that our explanation for the B2-phase nucleation suggests that a critical role is played by the MIL, consisting of a solid solution of Al in Fe and of Al-rich regions, in the nucleation of the B2 phase. Without the presence of this interface layer, the initial step of the atomic mixing would be controlled by the mobility of Fe atoms in Al, which is in fact higher than the mobility of Al in Fe, as suggested by the difference in their activation

energies, 2.3 eV [29] and 3.17 eV [30], respectively (neglecting the grain-boundary diffusion contribution). Consequently, we should observe the formation of a MIL composed of Al-containing Fe and then the formation of an Al-rich phase. However, we do not observe any evidence of phases different from the B2 one.

Our results are very different from those obtained by Csanády *et al* [31] in a study on the phase formation induced by thermal treatment in Fe–Al multilayer systems. The authors deposited an Fe (2 nm)/Al (8 nm) multilayer (19 at.% Fe) and observed the formation of an icosahedral phase together with the metastable Al_6Fe phase at temperatures higher than 523 K and the formation of Al_3Fe above 773 K. The different behaviour is probably related to the very small Fe grain size in the system of Csanády *et al*: their system could be considered, in fact, as a composite structure in which the Fe grains are embedded in an aluminium matrix and the nucleation of Al-rich phases is due to the presence of large interface areas.

4.2. Structural order in the B2 phase

The B2 FeAl phase is a body-centred-cubic derivative structure consisting of two interpenetrating simple cubic Bravais lattices: Fe atoms occupy one cubic lattice (the α-sublattice) and Al atoms the other (the β-sublattice). A perfectly ordered state for the B2 phase is possible only for a stoichiometric material: deviation from stoichiometry can be compensated for by either vacant lattice sites or by antisite atoms [32]. Fe atoms in antisite positions are mostly found in iron-rich alloys.

The solid-state reaction seems to be complete in the sample annealed at 673 K, the α-Fe sextet being absent in the corresponding spectrum of figure 2, while a certain proportion of structural defects persist, as indicated by the components used to fit the CEM spectrum in figure 4. This could be evidence of off-stoichiometry of the system [32] or could be indicative of an incomplete kinetics. As indicated by RBS analysis, the first possibility can be ruled out.

In order to check whether the observed spectral components added to the typical B2 singlet are an indication of residual defects in the B2 phase, we have subjected one sample to a longer heat treatment (80 h) at a higher temperature (773 K). The doublet and associated singlet decrease in intensity, as shown in figure 4, and we can conclude that the removal of structural defects in the B2 phase is a slow process even at 773 K.

5. Conclusions

In the present investigation we studied the structural evolution and phase formation in Fe–Al thin-film multilayers with average 1:1 atomic composition. The as-deposited multilayer sample presents mixed interface layers (MIL) a few nm thick, consisting of a diluted solid solution of Al in Fe and of Fe in Al. UHV heat treatments, at temperatures lower than 473 K, induce Al atomic migration to the MIL region without formation of any definite FeAl phase. Thermal annealing at 573 K induces the nucleation and growth of a defected B2 FeAl phase. The nucleation of the B2 phase cannot be explained just in terms of chemical driving forces or diffusional processes, but we have proved that the MIL in the as-deposited sample plays a critical role; see figure 5. Once formed, the defected B2 phase is thermodynamically stable also for higher treatment temperatures (773 K) and evolves slowly into a more ordered structure. Such structural order and the large size ($\sim$50 nm) of the FeAl crystalline grains indicate the synthesis of material of good quality.

Work is in progress to analyse the kinetics of FeAl B2 phase formation by studying the behaviour of multilayer samples with different Fe and Al layer thicknesses and by using complementary techniques such as transmission electron microscopy (TEM).

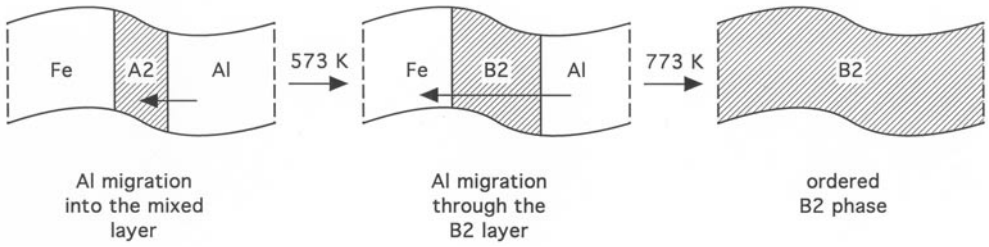

Figure 5. A schematic diagram showing the different stages which take the as-deposited Fe–Al multilayers to the final B2 phase.

Acknowledgments

The authors would like to thank C Armellini (Istituto Trentino di Cultura) for the XRD analysis and D Boscarino (Istituto Nazionale di Fisica Nucleare, INFN) for the RBS analysis. This work received specific financial support from the Istituto Nazionale per la Fisica della Materia (INFM).

References

[1] Kattner U R 1990 *Binary Alloy Phase Diagrams* ed T B Massalski (Metals Park, OH: ASM International) p 147
[2] Hultgren R, Desai P D, Hawkins D T, Gleiser M and Kelley K K 1973 *Selected Values of the Thermodynamic Properties of Binary Alloys* (Metals Park, OH: American Society for Metals) p 156
[3] Deevi S C and Sikka V K 1996 *Intermetallics* **4** 357
[4] McKamey C G, DeVan J H, Tortorelli P F and Sikka V K 1991 *J. Mater. Res.* **6** 1779
[5] *Iron Aluminides: Alloy Design, Processing, Properties and Applications* 1998 *Mater. Sci. Eng.* A **258**
[6] Miracle D B 1993 *Acta Metall. Mater.* **41** 649
[7] Ng H P, Meng X K and Ngan A H W 1998 *Scr. Mater.* **39** 1737
[8] Ishida M, Yuda S, Kamigaki K, Terauchi H, Hiyamizu S and Sano N 1992 *Surf. Sci.* **267** 54
[9] Harper J M E and Rodbell K P 1997 *J. Vac. Sci. Technol.* B **15** 763
[10] Shibaya H and Fukuda I 1997 *IEEE Trans. Magn.* **13** 1029
[11] Takahashi M, Kato N, Sato T and Wakiyama T 1987 *IEEE Trans. Magn.* **23** 3068
[12] Umesaki M, Yokuda Y and Hamanaka K 1982 *IEEE Trans. Magn.* **18** 1182
[13] Noetzel J, Brand K, Geisler H, Gorbunov A, Tselev A, Wieser E and Moeller W 1999 *Appl. Phys.* A **68** 497
[14] Meyer D C, Richter K, Paufler P, Gawlitza P and Holz T 2000 *J. Appl. Phys.* **87** 7218
[15] Shao G and Tsakiropoulos P 2000 *Phil. Mag.* A **80** 693
[16] *JCPDS* file No 4-787
[17] *JCPDS* file No 6-696
[18] Doolittle L R 1985 *Nucl. Instrum. Methods* B **9** 334
[19] Nasu S, Gonser U and Preston R S 1980 *J. Physique Coll.* C1 385
[20] *JCPDS* file No 33-20
[21] Rothhaar U, Oechsner H, Scheib M and Mueller R 2000 *Phys. Rev.* B **61** 974
[22] Bené R W 1982 *Appl. Phys. Lett.* **41** 529
[23] Majni G, Nobili C, Ottaviani G, Costato M and Galli E 1981 *J. Appl. Phys.* **52** 4047
[24] Geilman T, Chevallier J, Fanciulli M, Weyer G, Nevolin V and Zenkevitch A 1997 *Appl. Surf. Sci.* **109/110** 570
[25] Meyer M, Mendoza Zélis L, Sánchez F H and Traverse A 1994 *Hyperfine Interact.* **83** 327
[26] Tu K N, Ottaviani G, Thompson G D and Mayer J W 1982 *J. Appl. Phys.* **53** 4406
[27] Tu K N, Chu W K and Mayer J W 1975 *Thin Solid Films* **25** 403
[28] Eggersmann M and Mehrer H 2000 *Phil. Mag.* **80** 1219
[29] Mantl S, Petry W, Schroeder K and Vogl G 1983 *Phys. Rev.* B **27** 5313
[30] Hirvonen J and Raisanen J 1982 *J. Appl. Phys.* **53** 3314
[31] Csanády A, Guenter J R, Barna P B and Mayer J 1988 *Thin Solid Films* **167** 203
[32] Fu C L, Ye Y Y, Yoo M H and Ho K H 1993 *Phys. Rev.* B **48** 6712